Biomedical Optics EXPRESS

Coherence-gated Doppler: a fiber sensor for precise localization of blood flow

Chia-Pin Liang,[1] Yalun Wu,[2] Joe Schmitt,[3] Paul E. Bigeleisen,[4] Justin Slavin,[5] M. Samir Jafri,[6,7] Cha-Min Tang,[6,7] and Yu Chen[1,2,*]

[1]*Fischell Department of Bioengineering, University of Maryland, College Park, MD 20742, USA*
[2]*Department of Electrical and Computer Engineering, University of Maryland, College Park, MD 20742, USA*
[3]*St. Jude Medical, Inc., Westford, MA 01886, USA*
[4]*Depatment of Anesthesiology, University of Maryland School of Medicine, Baltimore, MD 21201, USA*
[5]*Department of Neurosurgery, University of Maryland School of Medicine, Baltimore, MD 21201, USA*
[6]*Department of Neurology, University of Maryland School of Medicine, Baltimore, MD 21201, USA*
[7]*Research Service, Baltimore VA Medical Center, Baltimore, MD 21201, USA*
**yuchen@umd.edu*

Abstract: Miniature optical sensors that can detect blood vessels in front of advancing instruments will significantly benefit many interventional procedures. Towards this end, we developed a thin and flexible coherence-gated Doppler (CGD) fiber probe (O.D. = 0.125 mm) that can be integrated with minimally-invasive tools to provide real-time audio feedback of blood flow at precise locations in front of the probe. Coherence-gated Doppler (CGD) is a hybrid technology with features of laser Doppler flowmetry (LDF) and Doppler optical coherence tomography (DOCT). Because of its confocal optical design and coherence-gating capabilities, CGD provides higher spatial resolution than LDF. And compared to DOCT imaging systems, CGD is simpler and less costly to produce. In vivo studies of rat femoral vessels using CGD demonstrate its ability to distinguish between artery, vein and bulk movement of the surrounding soft tissue. Finally, by placing the CGD probe inside a 30-gauge needle and advancing it into the brain of an anesthetized sheep, we demonstrate that it is capable of detecting vessels in front of advancing probes during simulated stereotactic neurosurgical procedures. Using simultaneous ultrasound (US) monitoring from the surface of the brain we show that CGD can detect at-risk blood vessels up to 3 mm in front of the advancing probe. The improved spatial resolution afforded by coherence gating combined with the simplicity, minute size and robustness of the CGD probe suggest it may benefit many minimally invasive procedures and enable it to be embedded into a variety of surgical instruments.

OCIS codes: (170.4500) Optical coherence tomography; (170.3340) Laser Doppler velocimetry; (280.1415) Biological sensing and sensors.

References and links

1. T. Grau, R. W. Leipold, R. Conradi, E. Martin, and J. Motsch, "Efficacy of ultrasound imaging in obstetric epidural anesthesia," J. Clin. Anesth. **14**(3), 169–175 (2002).
2. D. Karakitsos, N. Labropoulos, E. De Groot, A. P. Patrianakos, G. Kouraklis, J. Poularas, G. Samonis, D. A. Tsoutsos, M. M. Konstadoulakis, and A. Karabinis, "Real-time ultrasound-guided catheterisation of the internal jugular vein: a prospective comparison with the landmark technique in critical care patients," Crit. Care **10**(6), R162 (2006).
3. K. Wårdell, P. Blomstedt, J. Richter, J. Antonsson, O. Eriksson, P. Zsigmond, A. T. Bergenheim, and M. I. Hariz, "Intracerebral microvascular measurements during deep brain stimulation implantation using laser Doppler perfusion monitoring," Stereotact. Funct. Neurosurg. **85**(6), 279–286 (2007).
4. H. C. Eun, "Evaluation of skin blood flow by laser Doppler flowmetry," Clin. Dermatol. **13**(4), 337–347 (1995).

#184247 - $15.00 USD Received 28 Jan 2013; revised 23 Mar 2013; accepted 23 Mar 2013; published 24 Apr 2013

5. K. Kijsamanmith, S. Timpawat, N. Vongsavan, and B. Matthews, "Pulpal blood flow recorded from human premolar teeth with a laser Doppler flow meter using either red or infrared light," Arch. Oral Biol. **56**(7), 629–633 (2011).
6. A. L. Petoukhova, W. Steenbergen, and F. F. M. de Mul, "Path-length distribution and path-length-resolved Doppler measurements of multiply scattered photons by use of low-coherence interferometry," Opt. Lett. **26**(19), 1492–1494 (2001).
7. B. Varghese, V. Rajan, T. G. Van Leeuwen, and W. Steenbergen, "In vivo optical path lengths and path length resolved doppler shifts of multiply scattered light," Lasers Surg. Med. **42**(9), 852–860 (2010).
8. Z. P. Chen, T. E. Milner, S. Srinivas, X. J. Wang, A. Malekafzali, M. J. C. van Gemert, and J. S. Nelson, "Noninvasive imaging of in vivo blood flow velocity using optical Doppler tomography," Opt. Lett. **22**(14), 1119–1121 (1997).
9. V. X. D. Yang, M. L. Gordon, B. Qi, J. Pekar, S. Lo, E. Seng-Yue, A. Mok, B. C. Wilson, and I. A. Vitkin, "High speed, wide velocity dynamic range Doppler optical coherence tomography (Part I): System design, signal processing, and performance," Opt. Express **11**(7), 794–809 (2003).
10. V. Westphal, S. Yazdanfar, A. M. Rollins, and J. A. Izatt, "Real-time, high velocity-resolution color Doppler optical coherence tomography," Opt. Lett. **27**(1), 34–36 (2002).
11. Z. P. Chen, Y. H. Zhao, S. M. Srinivas, J. S. Nelson, N. Prakash, and R. D. Frostig, "Optical Doppler tomography," IEEE J. Sel. Top. Quantum Electron. **5**(4), 1134–1142 (1999).
12. R. Leitgeb, C. K. Hitzenberger, and A. F. Fercher, "Performance of Fourier domain vs. time domain optical coherence tomography," Opt. Express **11**(8), 889–894 (2003).
13. S. K. Piechnik, P. A. Chiarelli, and P. Jezzard, "Modelling vascular reactivity to investigate the basis of the relationship between cerebral blood volume and flow under CO_2 manipulation," Neuroimage **39**(1), 107–118 (2008).
14. V. Rajan, B. Varghese, T. G. Van Leeuwen, and W. Steenbergen, "Review of methodological developments in laser Doppler flowmetry," Lasers Med. Sci. **24**(2), 269–283 (2009).
15. J. M. Gardin, C. S. Burn, W. J. Childs, and W. L. Henry, "Evaluation of blood flow velocity in the ascending aorta and main pulmonary artery of normal subjects by Doppler echocardiography," Am. Heart J. **107**(2), 310–319 (1984).
16. D. Morofke, M. C. Kolios, I. A. Vitkin, and V. X. D. Yang, "Wide dynamic range detection of bidirectional flow in Doppler optical coherence tomography using a two-dimensional Kasai estimator," Opt. Lett. **32**(3), 253–255 (2007).

1. Introduction

Detecting blood vessels in front of a surgical probe in real-time is an important capability during interventional procedures. This may provide the ability to minimize laceration of vessels during stereotactic neurosurgery, avoid vessels during local anesthesia procedures deep inside the body, and locate vessels during central venous/arterial cannulation. Ultrasound is currently used for real-time image guidance and blood vessel localization for some of these interventional procedures. However, in some cases, such as neuraxial blockade, ultrasound guidance is especially challenging because of the complex encasement of bones that allows only a very narrow acoustic window for the ultrasound beam [1]. Furthermore, the guidance efficacy in some cases is still unsatisfactory due to limited resolution (~1 mm) and the need for complex hand-eye coordination [2]. Optical sensors that can be integrated with surgical tools and detect blood vessels in front of instruments provide a solution to these challenges.

An effective optical sensor needs to be small, flexible and rugged for integration with minimally invasive instruments. It also needs to have high lateral resolution (< 100 μm) to detect clinically significant blood vessels. Ideally, it should also have sufficient axial detection range to detect blood vessels millimeters ahead. Various optical technologies have been developed to monitor the blood flow. Laser Doppler flowmetry (LDF) has been used in neurosurgery [3], dermatology [4] and dentistry [5] to collect blood flow information. However, the resolution (mm-cm) of the two fiber design in a conventional LDF system is too coarse to allow location and avoidance of many vessels in the brain. Petoukhova *et al.* improved the axial resolution of LDF to 50 μm by using coherence-gating effect [6]. Although this approach successfully obtained depth-resolved information from the human skin [7], the lateral resolution is not sufficient (few mm [6]) for neurosurgery. Also the two fiber design with wide separation in LDF system is not compatible with minimally invasive procedures. In contrast, Doppler optical coherence tomography (DOCT) creates a very small imaging spot (10 μm) with a single fiber [8]. By scanning this spot, the flow information in the region of

#184247 - $15.00 USD Received 28 Jan 2013; revised 23 Mar 2013; accepted 23 Mar 2013; published 24 Apr 2013

interest (ROI) can be mapped out with great resolution. However, in many clinical applications, it is not necessary to obtain high resolution images of blood vessels and accept the tradeoffs associated with imaging. Often what is needed is simply to determine whether there is a blood flow at a precise location in front of a surgical probe. We developed a technology to serve in such situations.

Coherence-gated Doppler (CGD) is a real-time movement sensing technology that can be thought of as a hybrid between optical coherence tomography (OCT) and LDF. The system design is derived from time-domain DOCT or optical Doppler tomography (ODT) [8] with several important simplifications and modifications. By converting the DOCT imaging system to the CGD sensing system, the reference phase modulator, reference path length scanning, signal digitization and demodulation processing can be omitted. CGD only requires a simple electronic circuit to convert the Doppler beating signal to an audio signal. From the pitch and volume of the audio signal, we demonstrate that the simple CGD system enables us to differentiate tissue, vein and artery in live animals and also demonstrate that the CGD probe can potentially predict the creation of hematomas in neurosurgery.

2. Materials and methods

2.1 System setup

Figure 1A illustrates the design of the CGD system. The light source is a superluminescent diode (SLD) at 1310 nm (Qphotonics QFLD-1300-10S).The wavelength bandwidth of the light source is 3 nm, and thus the coherence length is 190 μm in water. The fiber (FC) coupler splits the photons to sample (90%) and reference arms (10%). The optical fiber circulator sends the illumination light from port 1 to port 2 and the backscattering light from port 2 to port 3. Both back scattering light from the sample and the reference mirror go to another fiber coupler (50/50) and the photons from each arm are re-distributed to two output fibers. The interference fringe from output fibers go to a dual balanced detection system, which rejects the common mode noise. After further amplification and frequency filtering (10 –20,000 Hz), the electronic signal is converted to an audio signal and broadcast by a speaker. We also collect the signal by a data acquisition (DAQ) card (National Instrument NI-6259) and process it with a computer (optional). The sampling rate of data acquisition is 400 kHz. The fiber probe consists of a single mode fiber (SM) and a GRIN multimode fiber (GM) for focusing (St. Jude Medical). The focal distance is 1.5 mm and the lateral resolution is 40 μm.

2.2 Design concept

The major differences between CGD (Fig. 1A) and DOCT (Fig. 1B) are indicated by the blue arrows. Firstly, we used a light source with a longer coherence length and extended the axial dimension of the detection volume from ~10 μm to 190 μm. By covering a larger detection volume, we can acquire ensemble information from the ROI and omit the requirement to scan the reference mirror. Secondly, we further extended the detection volume by omitting the phase modulation, which is commonly used in time-domain DOCT system [8–10]. The phase modulator in DOCT (Fig. 1B) enables heterodyne detection and rejects the self-beating signal (the interference between sample photons). Equation (1) shows more details:

$$I \sim \left|E_R + E_S\right|^2 = E_R E_R^* + E_S E_S^* + 2\,\mathrm{Re}\left(E_R E_s^*\right) = I_R + I_{\mathrm{hom}} + I_{het} \qquad (1)$$

#184247 - $15.00 USD Received 28 Jan 2013; revised 23 Mar 2013; accepted 23 Mar 2013; published 24 Apr 2013

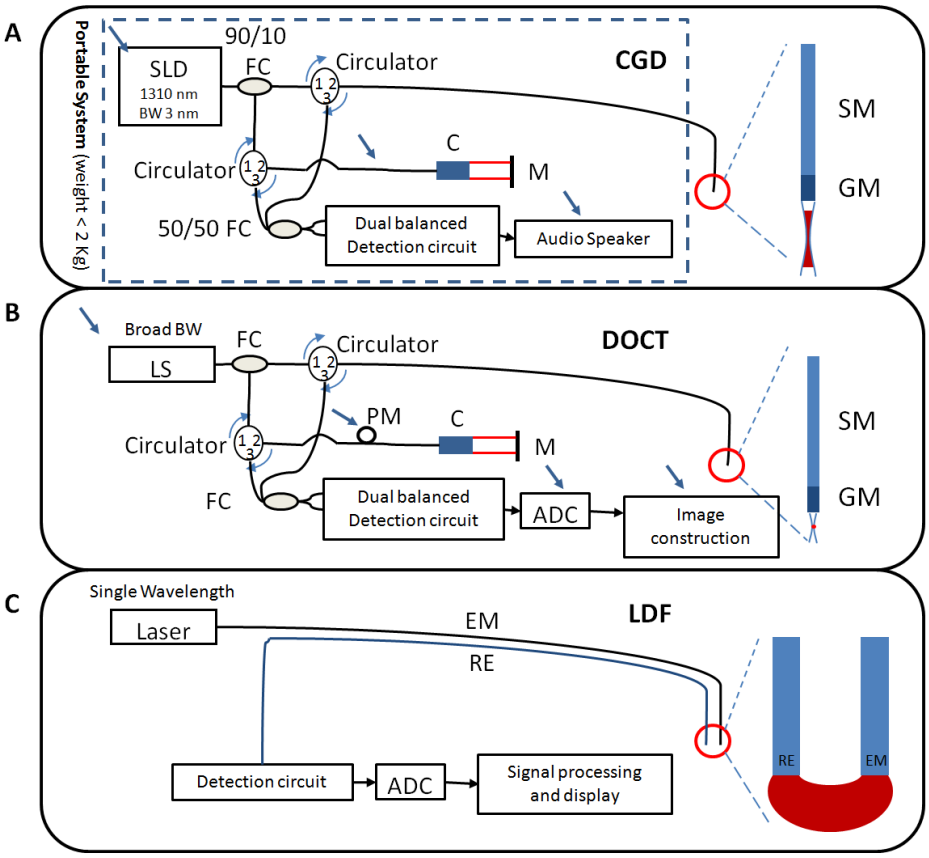

Fig. 1. (A) CGD system (B) Doppler OCT system (C) LDF system. SLD: superluminescent diode, LS: light source, BW: wavelength band-width, FC: fiber coupler, C: collimator, M: mirror, PM Phase modulator, ADC: analog to digital converter, SM: single-mode fiber, GM, gradient-index fiber, EM: emission fiber, RE, receiver fiber. The detection volume of each system is shown in the probe drawing to the right in red.

I is the intensity on the detector; E_R is the electric field from reference arm and E_s is the electric field from sample arm; I_R is the reference intensity coming from the interference between reference photons; I_{hom} is the homodyne intensity coming from the interference between sample photons (self beating signal); I_{het} is the heterodyne intensity coming from the interference between sample and reference photons. Because there is no Doppler shift between reference photons, I_R is a DC signal. On the other hand, due to the Doppler shift between sample photons and between sample and reference photons, I_{hom} and I_{het} are AC signals. In conventional time-domain OCT systems, due to the phase modulation in reference arm, I_{het} signal can be separated from the I_{hom} in frequency domain and I_{het} is the Doppler signal coming from the tissue within the coherence length surrounding the zero-delay plane. Therefore, if we select the heterodyne signal by frequency filtering, we can achieve high resolution flow imaging as demonstrated by ODT system [11]. In CGD system, we omit the phase modulation and do not intend to distinguish the I_{het} and I_{hom}. Therefore we receive all the Doppler signals accumulated in the illuminate path instead of just collecting the signal surrounding the zero-delay plane. In terms of its use for self-beating detection, CGD and LDF systems are similar; both collect Doppler signals accumulated along the illumination path. However, CGD has better spatial resolution than LDF (Fig. 1C) due to the confocal probe design and the SLD's shorter coherence length. Moreover, we can optimize the sensitivity by

#184247 - $15.00 USD Received 28 Jan 2013; revised 23 Mar 2013; accepted 23 Mar 2013; published 24 Apr 2013

tuning the reference power I_R [12]. Lastly, the interference fringe is directly converted to an audio signal without frequency demodulation. The frequency of the Doppler beating signal is proportional to the blood flow velocity: $\Delta f = \frac{2V\cos(\theta)}{\lambda}$. The velocity V of blood flow within medium-sized vessels is 10 mm/s [13]. The wavelength of light source λ used in the present study is 1.3 μm. The effective angle θ between the probe and blood flow varies, depending to the angle of approach, numerical aperture of the probe, and degree of multiple scattering within the tissue and blood. In practice, scattering within the tissue and blood ensures that the effective Doppler angle is never exactly 90 degrees, so that flow is detectable even with orthogonal orientation between the probe and a medium-sized vessel. The peak frequencies of the Doppler signal Δf are typically 0.1 - 15.4 kHz, which is within human audible bandwidth. Therefore, expensive data acquisition or any further data processing is not required to interpret the signal. We can directly identify the flow speed by the pitch of sound and the size of vessel by the volume of sound.

2.3 Data processing

The interference between two electric fields with Doppler frequency difference will generate a fluctuating AC signal, whose frequency is equivalent to the Doppler frequency difference. Therefore, the frequency of CGD waveform is equivalent to the Doppler frequency shift, which is linear proportional to the moving speed. The sign of signal does not reflect the flow direction. From the interference fringe, we can only measure the flow speed (the frequency) and the volume of moving scatters (the amplitude), but no information on the flow direction. To quantify the performance of the system, we record the interference fringe by a DAQ card (sampling rate 400 kHz) and calculate the M1 (first moment) factor, $\int \omega * P(\omega)\,\mathrm{d}\omega$ which is linearly proportional to the average concentration of the scatter multiplied by the root mean square of the velocity [14]. $P(\omega)$ is the power spectrum of the interference fringe. The power spectrum of the CGD waveform is calculated by taking Fourier transform and square the amplitude. The time domain window for Fourier transform is 0.1 second and the integration window on frequency domain is 0- 20 kHz. The M1 factor is used to characterize the linearity of speed measurement and detection volume. We also study the similarity of the time domain signal by autocorrelation. Firstly, we square the CGD waveform signal to avoid the cancelation between positive and negative signal. Then, we use the entire signal in the 5 seconds window to calculate the autocorrelation coefficient (Acorr) at different time shift (0-5 seconds). We also calculate the spectrogram from the CGD waveform. The theoretical minimum resolvable frequency is 0 Hz (DC) and the maximum resolvable Doppler frequency is 15MHz (3dB bandwidth), which is limited by the dual balanced detector (Thorlabs PDB145C). This frequency is corresponding to a flow speed of 9.75 m/s which is well above the fastest blood flow speed in human body (~1 m/s) [15]. In practice, the maximum frequency is determined by the sampling rate of data acquisition. In our study, the sampling rate is 400 kHz and thus the maximum frequency is 200 kHz (Nyquist limit). The minimum resolvable frequency is determined by the time window of short time Fourier transform (STFT), which is 0.1 second. Therefore, the resolution in frequency domain is 10Hz. The minimum (10 Hz) and maximum (200 kHz) frequency are corresponding to Doppler velocity of 0.0065 mm/s and 130 mm/s respectively. The signal frequencies within human audible range (< 20 kHz) are displayed. A median filter is applied to improve visualization.

2.4 Capillary phantom

We constructed a vessel phantom by injecting 2% Intralipid solution through a capillary tube (I.D. = 0.4 mm), with the flow speed controlled by a motorized pump (Newport CMA-25CCCL). The velocity dynamic range, limited by the pump system, was 0.2-5 mm/s.

#184247 - $15.00 USD Received 28 Jan 2013; revised 23 Mar 2013; accepted 23 Mar 2013; published 24 Apr 2013

2.5 In vivo rat femoral vessel detection

All animal procedures were approved by the Institutional Animal Care and Use Committee (IACUC) at the University of Maryland, and animals were treated in accordance with the PHS Policy on Humane Care and Use of Laboratory Animals, the National Institutes of Health Guide for the Care and Use of Laboratory Animals, and the Animal Welfare Act (7 U.S.C. et seq.). Anesthetized (ketamine 50 mg/kg and xylazine 5 mg/kg, intraperitoneal) Sprague-Dawley rats (n = 2, male, wt. ~400 g) in supine position have their femoral vessels exposed. The blood vessel color and relative position to the femoral nerve allow visual identification of the artery and vein. We place the CGD probe 3 mm away from the exposed vessels and translated the probe laterally to acquire information from tissue, vein and artery. The audio signal is recorded by a voice recorder (Sony, ICD-PX720).

2.6 In vivo deep sheep brain vessel detection

The effectiveness of the CGD probe was evaluated by examining its ability to detect vessels below the surface of the male sheep brain (wt. ~100 kg). Anesthesia is induced with 5 mg/kg ketamine (IV) and maintained under 1-4% isoflurane in 100% oxygen. After the sheep is deeply anesthetized, craniotomy is performed. The dura and pia membrane on the surface are carefully removed. Then, the CGD probe is inserted by hand. The inset of Fig. 2 shows the CGD probe placed in a 30 G needle and Fig. 2 shows the picture of a CGD probe being inserted into sheep brain *in vivo*. We also placed an US probe (Edge model, FUJIFILM SonoSite, Inc.), directly on top of the brain tissue to monitor the relative position between CGD probe and blood vessels. The US images are synchronized with CGD audio by the corresponding time marks.

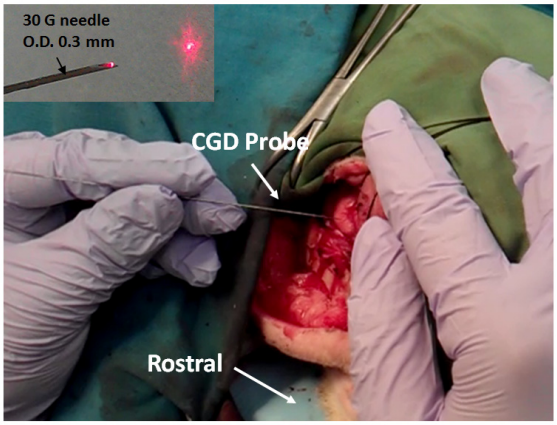

Fig. 2. A CGD probe during insertion into sheep brain. The inset shows a CGD probe placed in a 30 G needle.

3. Results

3.1 CGD system characterization

Figure 3 shows the linearity of the flow speed, as measured by the capillary phantom. CGD shows good linearity and the R-squared value is very close to 1. We also tested whether the CGD probe can resolve a capillary in a highly scattering environment. The vessel phantom was immersed in 2% Intralipid solution, and the flow speed parallel to the probe is 1.5 mm/s. The inset of Fig. 4A shows the DOCT B-scan image of the capillary. We scanned the CGD probe across the vessel and Fig. 4A shows the CGD probe can easily profile the parabolic flow in this 0.4 mm capillary (CGD probe is 0.4 mm away from the top surface of capillary). This result shows the great targeting capability of a CGD probe in a highly scattering

#184247 - $15.00 USD Received 28 Jan 2013; revised 23 Mar 2013; accepted 23 Mar 2013; published 24 Apr 2013

environment. Also we characterized the axial detection range by placing the CGD probe at different axial positions from the capillary (Fig. 4B). At the zero point, the CGD probe contacted the capillary and signal is close to the background signal level. From 0.18 - 0.71 mm the signal is significantly higher than the background level.

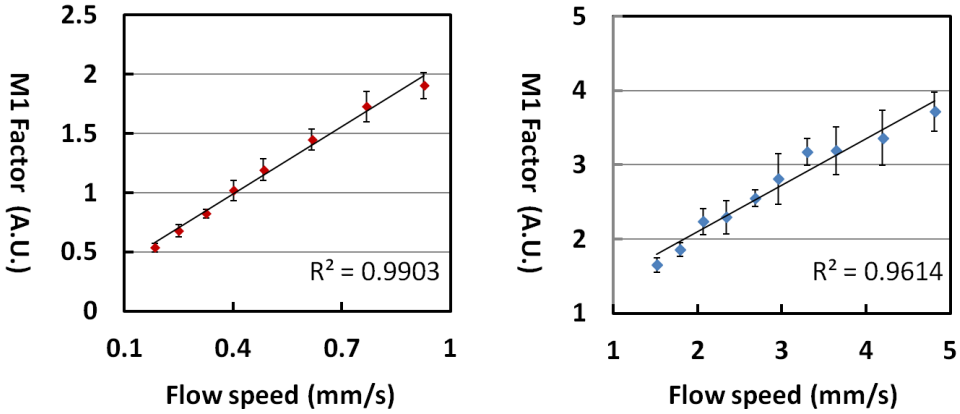

Fig. 3. Characterization of the linearity of flow speed measurement within two ranges.

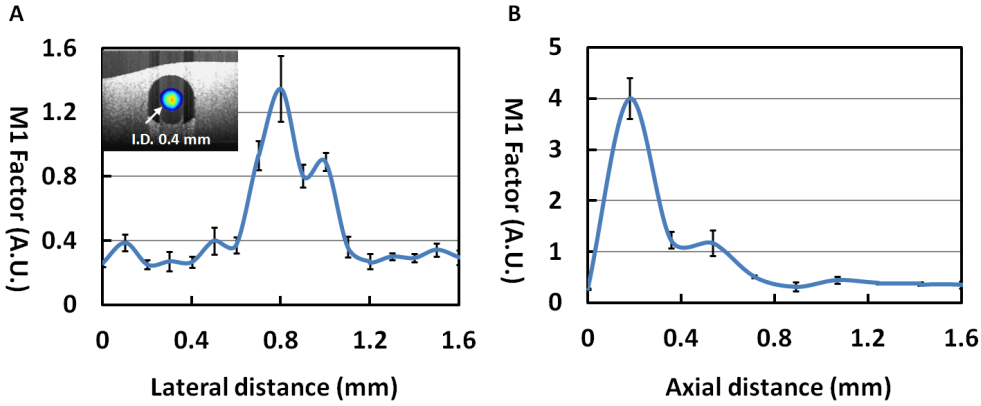

Fig. 4. (A) Signals measured while scanning the CGD probe (0.4 mm away from the top surface of capillary) laterally across a capillary tube immersed in 2% Intralipid solution. The inset shows a DOCT B-scan image of the phantom. The flow speed in the capillary is 1.5 mm/s parallel to the CGD probe. (B) Axial detection range. Moving a CGD probe axially away from a capillary immersed in 2% Intralipid solution.

3.2 Rat femoral vessel flow measurements

To test the feasibility of vessel detection and differentiation, we place the CGD probe on top of the exposed rat femoral vessels (Fig. 5A). The femoral artery and vein can be clearly distinguished by their appearance (i.e. color, size, and pulsatile movement). They are separated from each other by 1 mm. The CGD signals of the muscle tissue, vein and artery are also clearly apparent (Fig. 5B-D). Because the surrounding muscle tissue is not moving, its Doppler signal shows few high frequency components. After DC filtering, it has much smaller amplitude than the signal from the vessels. Also, we can see that the bulk motion generated a sharp peak, which represents large volume of scatter moving all together. The signal from the vein (Fig. 5C) shows steady flow of blood cells, with frequency characteristics different from those of the pulsating artery (Fig. 5D). The pulsating voltage represents the variation of the volume of moving blood cells during a pulsation cycle. The difference between tissue, vein and artery is even more apparent from their audio signals (Fig. 5 (Media 1)). Note that the CGD probe can easily differentiate two vessels that are only 1 mm apart at the distance 3 mm

#184247 - $15.00 USD Received 28 Jan 2013; revised 23 Mar 2013; accepted 23 Mar 2013; published 24 Apr 2013

away from the sample. This result demonstrates that the CGD probe can differentiate the neighboring vessels at a distal location far from the zero-delay plane (the zero-delay plane is matched with the focal plane at 1.5 mm distance from the fiber surface). Unlike heterodyne detection which can only obtain the signal close to the zero-delay plane, homodyne detection enables us to obtain the signal along the illumination path. This capability provides us longer buffer distance before hitting the vessel, which can be beneficial for avoiding hemorrhage. The amplitude of artery is smaller than vein. This is probably due to the thicker arterial wall.

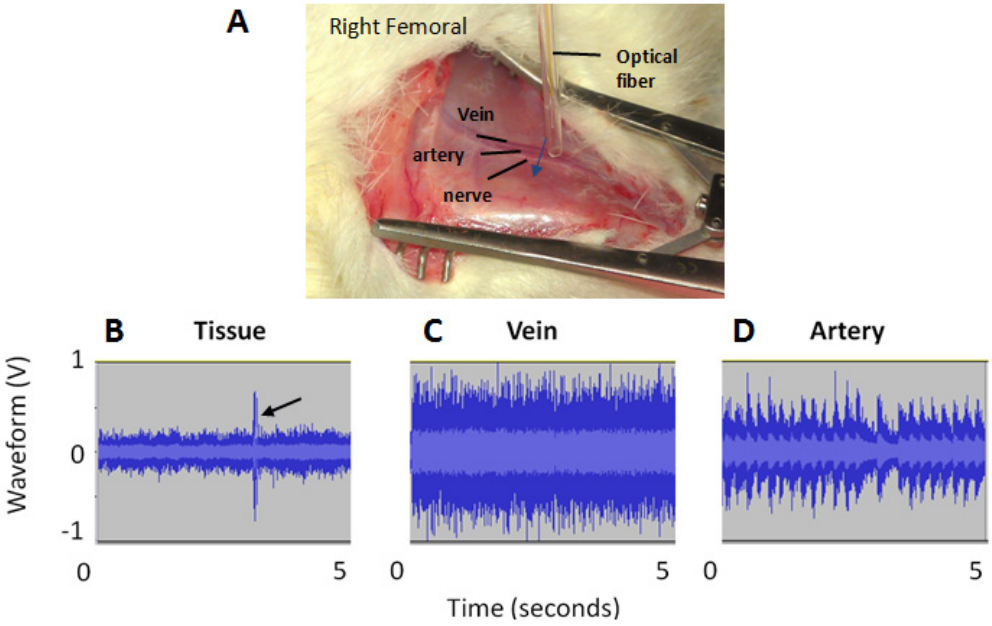

Fig. 5. (A) Exposed rat femoral vessels and CGD probe inside a large outer guide. CGD probe is 3 mm away from the sample. Voltage waveform (Media 1) from (B) rat femoral tissue, (C) vein, and (D) artery. Arrow indicates bulk motion.

3.3 Sheep brain vessel detection

Next, we tested the performance of the CGD needle probe (Fig. 2) for detecting vessels deep in the sheep brain. Figure 6 shows the voltage waveform and the spectrogram from tissue (Fig. 6A), vein (Fig. 6B), and artery (Fig. 6C). When the CGD probe is surrounded by highly scattering brain tissues, any relative motion between the probe and the brain generates very strong Doppler signal. The spectrogram shows that the signal is strong (large volume of scatters) with focused frequency range (uniform speed). In contrast, the signal from a vein is more homogeneous in the frequency domain. The waveform of an artery shows the pulsation pattern, and the spectrogram reveals the speed variation during a pulsation cycle. When the bulk motion (tissue movement with respect to the CGD probe during insertion) signal is mixed with the artery signal, it may be challenging to differentiate them in the spectrogram. However, if we study the similarity of the time domain signal by autocorrelation, we can see the clear difference between the bulk motion and the artery. We find that the difference of the frequency distribution between different spikes in the bulk motion spectrogram generates irregular fluctuation on Acorr, which is distinctively different from the periodic Acorr of the artery. In Fig. 6A, from 4.5 second to 5 second (indicated by the red arrows), the probe is static and the bulk motion is significantly lower than the signal in other time period. Acorr of the vein remains in a constant level due to the homogeneity of the signal. As it is with the femoral vessels, it is easier to differentiate between bulk motion, vein and artery by their characteristic pitch or pulsating patterns from the audio signal (Fig. 6 (Media 2)).

#184247 - $15.00 USD Received 28 Jan 2013; revised 23 Mar 2013; accepted 23 Mar 2013; published 24 Apr 2013

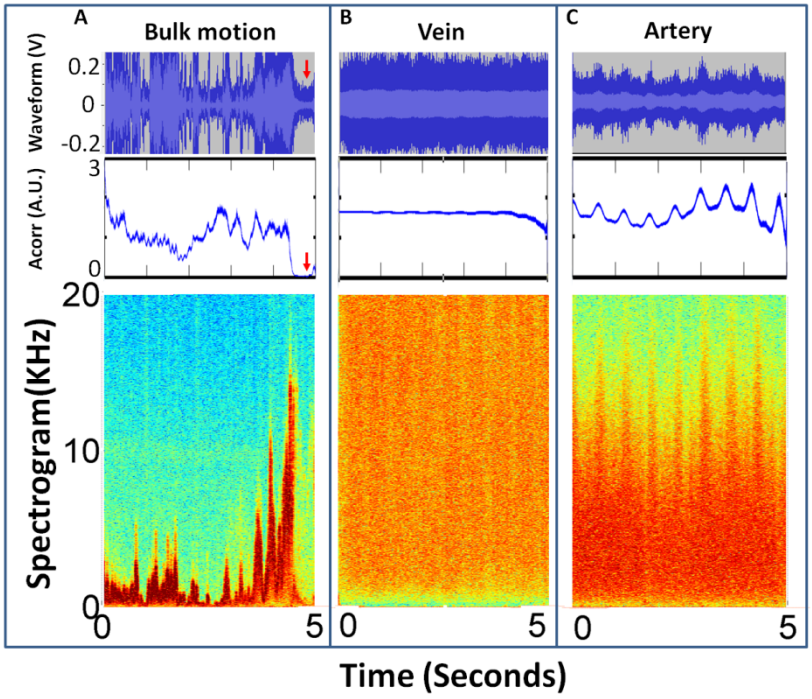

Fig. 6. The CGD waveform (Media 2), autocorrelation coefficient and spectrogram of (A) advancing probe in brain tissue, (B) vein, and (C) artery in sheep brain in vivo. The red arrows indicate the time point when the CGD probe is static relative to the brain tissue.

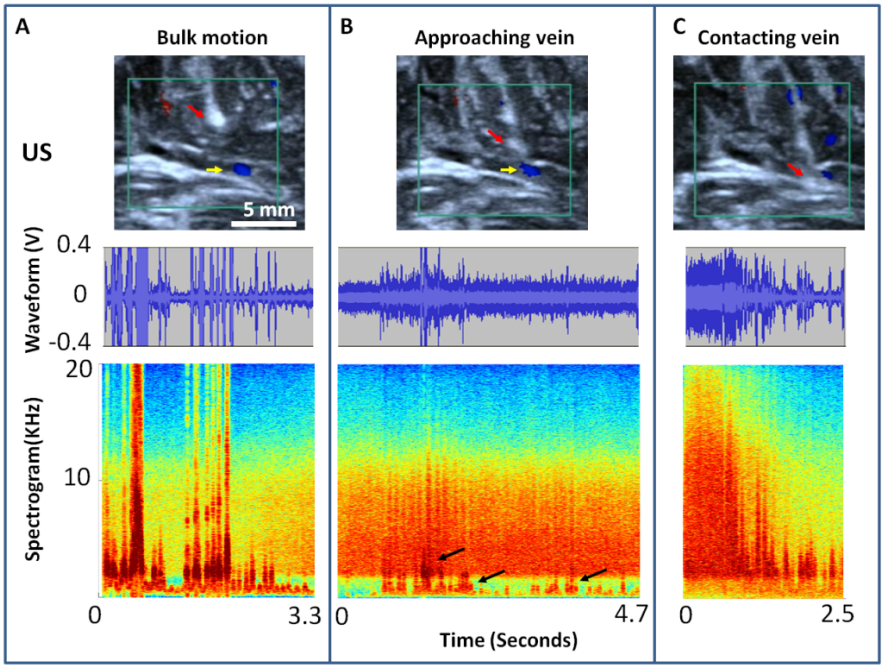

Fig. 7. Ultrasound monitoring with Doppler detection of the CGD probe as it approaches a vessel (yellow arrows) in a sheep brain *in vivo* (Media 3). The CGD probe tip appears as the bright white spot (red arrows). The target vein is the blue spot in the insets in top panel. (A) Bulk motion away from the vein, (B) approaching the vein, and (C) pressing on the vein resulting in the disappearance of the ultrasound Doppler signal as well as the CGD signal.

#184247 - $15.00 USD Received 28 Jan 2013; revised 23 Mar 2013; accepted 23 Mar 2013; published 24 Apr 2013

3.4 US-guided CGD vessel detection

To verify that the CGD probe can detect blood vessels in highly scattering tissues, we pushed a CGD probe toward a blood vessel in the sheep brain under US guidance. Figure 7A shows the situation when the probe (indicated by red arrow) is 1-4 mm away from the vessel (indicated by yellow arrow). The signal is dominated by bulk motion. The blood flow signal was initially detected at distance 3 mm in front of needle. Similar to the signal from the femoral vessel data (Fig. 6A) the bulk motion has high intensity and focused frequency distribution. As the probe approaches the vessel (< 1mm), the blood flow signal shows a uniform frequency distribution (Fig. 7B). Figure 7B also shows that the blood flow signal was mixed with bulk motion signal (indicated by black arrows). Lastly, when the CGD probe comes in contact with the vessel the blood flow signal initially becomes stronger followed by a loss of the CGD flow signal. Figure 7 (Media 3) shows the US video synchronized with CGD audio. To help listeners recognize the blood flow signal of the vein a chime is provided in the audio to indicate the beginning of the detected signal. The probe is advanced until it constricts the flow and the ultrasound signal is lost; the CGD signal also attenuates. A second chime is provided as the flow signal attenuates.

4. Discussion

We have developed a thin (0.125 μm) and flexible CGD fiber probe that can detect at-risk blood vessels with real-time audio feedback up to 3 mm in front of advancing needle in brain tissue *in vivo*. The diffuse optics design of laser Doppler flowmetry (LDF) with sample volume in the mm to cm range often includes signal from surrounding tissues and thus is not ideal for applications required high spatial specificity. The CGD probe with confocal optics design enable us to target a 0.4 mm capillary (Fig. 4A) and differentiate blood vessels that are only 1 mm apart (Fig. 5). On the other hand, Doppler optical coherence tomography (DOCT) has high spatial resolution (~10 μm), high temporal resolution (40 Hz) and wide flow speed dynamic range (7 μm/s to 52 cm/s) [16], but it requires extensive post processing and an expensive system to obtain the high resolution images. In contrast, CGD is a simple, robust and low-cost sensing system, which provides an audio signal that is rich in content, yet is easy for the operator to interpret (Fig. 5 (Media 1) & Fig. 6 (Media 2)). Real-time temporal resolution (10 Hz) and broad electronic detection bandwidth (10- 20,000 Hz) allows us to differentiate the audio signals from artery, vein and motion artifact (Figs. 6 & 7).

In order to achieve the best balance between the depth sensitivity and resolution, we carefully choose the 190 μm coherence length (CL). In ideal case, we hope to detect a blood vessel few millimeters away with sub-mm lateral specificity. Shorter CL provides higher resolution but also limits the depth detection range. We have used an SLD with 43 nm bandwidth at 1.325 μm center wavelength and found that it can only detect a vessel within 60 μm depth range, which is too short to prevent hemorrhage. Therefore, we further relax the detection range to 0.5 mm (Fig. 4B) by increasing the CL to 0.19 mm. In the animal study, Fig. 7 (Media 3) shows that it can detect a blood vessel that is 3 mm away due to longer transportation mean free path in the brain. On the other hand, if we further relax the CL to mm level, it may further improve the depth detection range, but may also include diffuse photons from the background tissue resulting in poor spatial specificity. We have to maintain the lateral resolution at sub-mm level in order to avoid the millimeter-sized blood vessels. Therefore, a light source with CL close to the mean free path of scattering tissues (~0.1 mm [3]) provide us the best balance between the detection range and the resolution.

We also choose the confocal probe design for optimal depth sensitivity. Without beam focusing and the confocal effect, a collimated beam may allow us to detect a blood vessel further ahead. However, in the scattering tissues, most of signal obtained by a parallel emitting probe will be from the tissue that is immediate proximal to the probe surface. On the other hand, a focused beam can deliver higher intensity to the deep tissue and thus provide

#184247 - $15.00 USD Received 28 Jan 2013; revised 23 Mar 2013; accepted 23 Mar 2013; published 24 Apr 2013

better sensitivity at the distance further away from the probe. Therefore, a focused beam provides longer buffer distance before hitting the blood vessel than a collimated beam and thus has better chance to avoid hemorrhage.

CGD is best suited for situations that require multitasking rather than tasks requiring precise image guidance. As shown in Fig. 5B, if the probe is static relative to the tissue, the amplitude of audio signal is low. When the probe reaches blood vessels, a high volume of flowing scatterers generates a much louder signal, and the artery shows a clear pulsatile pattern. From the spectrum analysis (Fig. 6), we find that the bulk motion has a narrow frequency distribution, while the movement of red blood cells in vessels is associated with a more homogeneous frequency distribution. The audio signals from blood vessels are more like white noise, which is clearly distinctive from the loud chirpy sounds associated with needle insertion (Fig. 6 (Media 2)). The pulsatile nature of arterial flow clearly distinguish venous and arterial flow. Acorr analysis also shows the clear difference between bulk motion, vein and artery (Fig. 6). The downside of the Acorr analysis is that it requires a long time window (couple seconds) that includes several heart beats and thus it cannot be implemented in real-time system. However, in real surgery, most of instruments are advanced slowly and provide us long acquisition time. Also, since most of bulk motion signal are from the relative movement between the probe and the tissue, stopping the probe is actually the most effective way to suppress the bulk motion signal (Fig. 6A 4.5 to 5 seconds). Therefore, we envision that the probe should be advanced slowly if a suspicious vessel is detected and then we can use the Acorr to analyze whether it is a pulsating artery. We will perform more animal experiments in the future to evaluate the false positive rate.

One limitation of CGD is that it can only provide a semi-quantitative distance measurement based on the volume of audio signal. The strength of volume, however, also varies with the tissue scattering coefficient and the number of moving scatters. Therefore, we may detect blood vessels further away in the gray matter (low scattering) than in the white matter (highly scattering) and detect a large blood vessel further ahead than a small vessel. However, in the clinical settings, if there is a blood vessel with strong signal sitting ahead, we should stop the probe no matter how far it is from the vessel. In the future, we will perform more animal studies to determine the criteria for stopping the probe.

It is worth to note that CGD may not detect small vessel (~10 μm) at 90 deg angle when the probe is very close to the vessel. The mean free path (MFP) in brain tissue is around 0.15-0.3 mm [1]. Beyond this ballistic scattering regime, multiple scattering events effectively randomize the photon propagation direction resulting in random incident angles to the moving blood cells. Therefore, we should be able to detect the laminar flow from any angle at the distance > 0.3 mm to the blood vessel. When the probe is proximate to the vessel, however, the illumination becomes more directional and the effective incident angle depends on the scattering property of blood cells. If the diameter of the vessel is comparable to the MFP of blood (~7 μm [2]), we will not be able to acquire the Doppler signal at 90 degree. For vessel that is much larger than 7 μm, multiple scattering between blood cells will randomize the incident angle and enable us to acquire the Doppler signal from any angle. In the practical situation, we hope to stop the probe at the position > 0.3 mm away from the high-risk blood vessels that are millimeters in size. Under this circumstance, we should not encounter the angle issue.

CGD probe is a great complimentary technology to tomographic techniques. We can use the wide filed-of-view tomographic imaging such as ultrasound to deliver the CGD probe to the region of interest and perform precise targeting with high precision (<0.1 mm) CGD local information/feedback. Figure 7 (Media 3) shows that the CGD probe is capable of detecting blood vessels that are on average 3.4 ± 1.3 mm from the tip of the probe. With millimeters axial detection range and lateral tissue confinement, we can aim the probe to a brain vessel for tens of seconds (Fig. 7 (Media 3)).The signal was found to become stronger when the CGD probe contacted the blood vessel. Further advances of the CGD probe resulted in the loss of

#184247 - $15.00 USD Received 28 Jan 2013; revised 23 Mar 2013; accepted 23 Mar 2013; published 24 Apr 2013

both the CGD and the US Doppler signal and an ultrasound pattern suggestive of a hematoma is then formed in proximity to the blood vessel. On the other hand, many needle-based procedures are still performed without imaging guidance due to the limitations of technology. For example, in stereotactic neurosurgery, the skull blocks most of ultrasound signal and it is difficult to fit the ultrasound probe to the small opening along with surgical instruments. Therefore a thin CGD probe (<30 G) that can be easily integrated with surgical instruments and provide real-time feedbacks on local blood flow in front of the probe tip has great potential to improve the safety of these "blind" procedures. CGD probe is thin (~0.125 mm) and can be embedded within the outer tubing of the needle and can aim at the ROI by using forward or side viewing probes. Integrating fiber sensor with needle has been published previously [4]. A similar design can be adapted for CGD probes.

5. Conclusion

Coherence-gated Doppler (CGD) provides the means for detecting blood flow with higher spatial resolution and with a smaller, more robust probe than conventional laser Doppler flowmetry at a cost of shorter depth of view. This tradeoff favors interventional procedures that require insertion of thin probes deep into tissue and where small vessels need to be detected with high precision.

Acknowledgments

We thank Professor James Fujimoto from MIT and Professor Changhuei Yang from Caltech for insightful discussion, Dr. Chris Peterson from St. Jude Medical Inc. for providing the fiber probes, Dr. James Jiang from Thorlabs Inc. for technical assistance, Dr. Didier Depireux from UMD for data analysis and Dr. Zhongjun Wu from UMMC for assistance in animal experiments. This work is supported in part by the University of Maryland Baltimore (UMB) and College Park (UMCP) Seed Grant Program, the Nano-Biotechnology Award of the State of Maryland, the Prevent Cancer Foundation, A. Ward Ford Memorial Research Grant, NIH R21EB012215-01A1, R21DK088066-01A1, NSF CAREER Award CBET-1254743, VA Merit Reviews (C-M. T).